

RESEARCH PAPER

A wide Bandwidth Pyramidal Horn Antenna with Enhanced Gain Using Metasurface layer

Avin Jawhar Ali, and Rashad Hassan Mahmud

Department of Physics, College of Education, Salahaddin University- Erbil, Kurdistan Region, Iraq

ABSTRACT:

A new design of a pyramidal horn antenna operating at 8-18 GHz based on the waveguide structure is presented in this paper. A metasurface layer, which consists of a set of periodic unit cells, is employed on the *E*-plane walls of the horn antenna. This is to enhance the realised gain and bandwidth. The unit cell shape is chosen based on the cavity resonator theory. The design method of the unit cells is analyzed and presented here using the Computer Simulation Technology (CST) microwave studio. The scattering parameters of a single unit cell are optimised in order to operate it at the designed operating frequencies. Compared to a conventional pyramidal horn, the proposed horn antenna gain improves up to 10 dBi. The peak gain is 23.7 dBi and the reflection coefficient at $S_{11} = -10$ dB is 5%. The radiation patterns are well shaped, and are stable over a large operating frequency range. The proposed pyramidal horn antenna is relatively low profile and may be of interest in satellite communication systems.

KEY WORDS: Horn antenna, Metasurface, high gain, waveguides.

DOI: <http://dx.doi.org/10.21271/ZJPAS.33.6.6>

ZJPAS (2021) , 33(5);47-56.

1.INTRODUCTION :

Due to their capability in manipulating the Electromagnetic (EM) waves, metamaterial employments in the design of wireless communication components have increased recently (Chen et al., 2016, Asl et al., 2020, Abdulkarim et al., 2020). The periodic structure of the metamaterial, which couple and interact with the incident EM fields depending on the resonant frequencies, shows the features which are not existed in ordinary materials (Abdulkarim et al., 2020). Such features can be of use in the design and introduce new features to antennas. Usually, the antenna radiation patterns have a main lobe, which is utilised to launch the information to space, and some minor lobes.

These minor lobes are not desirable during the communication process. Thin layers of metasurface lenses are employed at the opening aperture of a pyramidal horn antenna in order to reduce the side lobe levels, improve the gain, and enhancing the impedance bandwidth (Chen and Ge, 2017, Wang et al., 2019, Moradi and Mohajeri, 2017). To improve the antenna gain without degrading other performances, a conical horn antenna is integrated with a Fabry-Perot resonant structure (Ge et al., 2016). An aperture antenna array feed by a pyramidal E-plane horn antenna is presented in (Li et al., 2019) using the 3D printing technology to confirm the capability of such technology in the design of large microwave circuit structure.

Circularly polarised feature of antennas are in demand in many modern communication systems in order to overcome the reflectivity and phasing issues. Metamaterial could be interest to yield this feature. A metasurface layer is employed in a pyramidal horn antenna to design a linear-to-circular polariser transformer and then obtain a

* Corresponding Author:

Avin Jawhar Ali
E-mail: Avin.ali@su.edu.krd

Article History:

Received: 24/08/2021
Accepted: 19/10/2021
Published: 20/10 /2021

circular polarised pyramidal horn antenna (Lin et al., 2018). Two dielectric slabs, which are covered by three metallic element arrays, are used to design a thin metasurface linear-to-circular polarisation converter (Ge et al., 2018). The converter placed on the aperture of the pyramidal horn is to convert the linearly polarised wave transmitted by the horn antenna to circularly polarised wave.

Metasurface structures are widely used to design low-profile, high gain, and wide bandwidth horn antennas. A cross-shaped resonator etched on a microstrip aperture, which is mechanically stable, is placed at the throat of horn to enhance the gain and bandwidth (Esselle, 2007). A 60 GHz H-plane horn antenna is designed using the micromachining technologies (Pan et al., 2009). The authors claim that the technology improves the efficiency and overcome the packaging issues. To reduce the weight and enhance the bandwidth, homogenous metamaterial liners is used in horn antenna designs to achieve hybrid mode (Lier and Shaw, 2008). As a practical implementation, an approach is presented in (Wu et al., 2010, Wu et al., 2012) for the design of hybrid mode conical horn antenna which maintains the balanced hybrid conditions. A metasurface based on dispersion engineered characteristics to design inhomogeneous hybrid mode horn antenna is presented in (Wu et al., 2013) to enhance the antenna bandwidth.

In this paper, a new design of a pyramidal horn antenna operating at the range 8-18 GHz is

presented. A novel periodic unit cell structure is demonstrated and placed on the electric plane (E-plane) of the horn. This is to enhance the antenna gain and bandwidth. The design method of the unit cell is analyzed. The proposed design could be of interest of satellite communication applications. This paper is organised as follows. The design method of a conventional pyramidal horn antenna is discussed in Section 2. The method is then utilised in Section 3-1 to synthesis a pyramidal horn antenna operating at range 8-18 GHz with the aid of the Computer Simulation Technology (CST). Later, in Section 3-2, the novel unit cell is transplanted on the E-plane of the pyramidal horn antenna. The results are analysed and discussed in Section 3-3. This is followed by the conclusions confined in Section 4.

2. ANTENNA DESIGN

The pyramidal horn is the one which is flared in both electric E - and magnetic H -planes, as shown in Fig. 1. In essence, its radiation characteristics can be considered as a combination of the E - and H -plane sectorial horns. Usually, the procedure of designing the pyramidal horn is to combine the results that were obtained for the E - and H -plane sectorial horn. A more precise mathematical formulation given in (Maybell and Simon, 1993) is used here in the design of the pyramidal horn antenna.

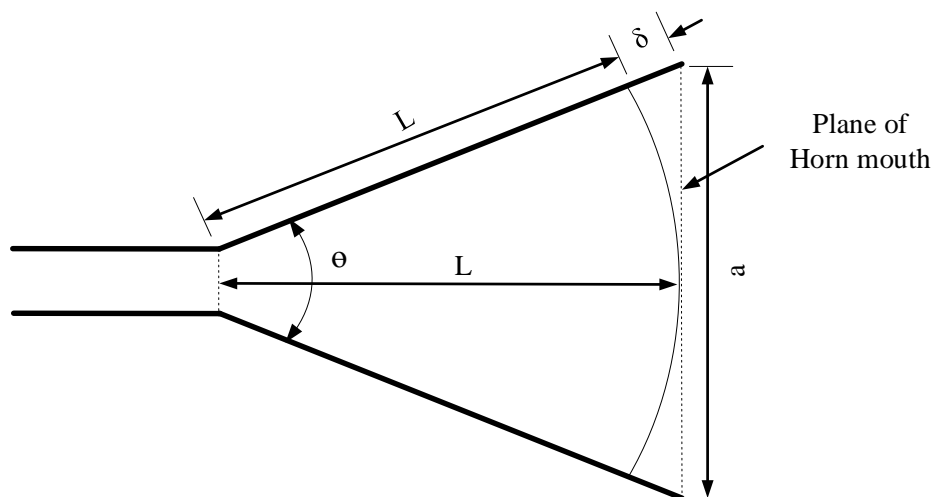


Figure 1: Cross section view of a Pyramidal horn antenna labeled with fundamental dimensions. (Marhefka and Kraus, 2002)

There is a simplified model to design and calculate the optimal dimension of the pyramidal horn antenna shown in Fig. 1 as follows:

$$\cos\left(\frac{\theta}{2}\right) = \frac{L}{L+\delta} \quad (1)$$

$$\sin\left(\frac{\theta}{2}\right) = \frac{a}{2(L+\delta)} \quad (2)$$

$$\tan\left(\frac{\theta}{2}\right) = \frac{a}{2L} \quad (3)$$

Where; θ = flare angle (θ_E for E -plane, θ_H for H -plane), a is aperture length (a_E for E -plane, a_H for H -plane), and L is horn length.

The value of phase error (δ) is very important in determining the performance of a horn antenna. δ is usually a sufficiently small fraction of a wavelength so that the field maintains nearly uniform phase over the entire aperture. As the conclusion drawn by (Chu and Barrow, 1939), there is always an optimum flare angle for which the directivity is a maximum for a constant horn length. This is not hard to understand. At first, assuming that δ is quite small and the horn length is constant, the directivity of the horn increases and half power beamwidth (HPBW) decreases as the aperture a and flare angle θ are increased. However, when the aperture and flare angle become so large that δ is equivalent to 180 electrical degrees, the field at the edge of the aperture is in opposite phase to the field on the axis. Therefore, when $\delta = 180^\circ$, the phase reversal at the edges of the aperture reduces the directivity and increases the side lobes. It turns out that the maximum directivity happens at the largest flare angle for which δ does not exceed a certain value

(δ_0). The value of δ_0 must usually be between 0.1 and 0.4 free-space wavelength (Marhefka and Kraus, 2002). In the E plane of the horn, δ is usually held to 0.25λ or less. However, in the H plane of the horn, δ can be larger or about 0.4λ because E field goes to zero at the horn edges (Marhefka and Kraus, 2002).

In general, a very long horn with a small flare angle is required in order to obtain an aperture distribution as uniform as possible. However, from the standpoint of practical convenience, the horn should be as short as possible. So, in this design, the horn length (L) is chosen to be 2λ to keep δ in range, and δ is 0.375λ (usually about 0.4λ). According to the equations (1), (2) and (3), the important parameters of the antenna can be determined at the centre frequency $f_0=13$ GHz (or $\lambda = c/f = 23.07$ mm, at free space) as follows:

$$\theta = 2 \cos^{-1}\left(\frac{L}{L+\delta}\right)=65.3^\circ$$

$$a_e = a_h = 2L \tan\left(\frac{\theta}{2}\right)=59.12 \text{ mm}$$

Now, the physical aperture area (A_p) can be computed for the antenna as follows;

$$A_p = a_e \times a_h = 3495.17 \text{ mm}^2$$

The HPBW also can be found by using the following expression;

$$HPBW = \frac{56^\circ}{a_{e\lambda}} = 21.87^\circ$$

Where $a_{e\lambda} = \frac{a_e}{\lambda} = 2.56$ is normalised free space wavelength aperture dimension.

The directivity (D) of a horn antenna can be obtained using (Marhefka and Kraus, 2002) as;

$$D = 4\pi \frac{A_e}{\lambda^2} = 4\pi \frac{\epsilon_{ap} A_p}{\lambda^2} \approx 7.5 \frac{A_p}{\lambda^2} \quad (4)$$

Where A_e is the effective aperture, A_p is physical aperture, ϵ_{ap} is aperture efficiency (≈ 0.6) (Marhefka and Kraus, 2002). According to (4), the D value of the horn antenna is calculated which is equal to:

$$D \approx 10 \log_{10} \left(7.5 \frac{A_p}{\lambda^2} \right) = 16.92 \text{ dBi.}$$

It should be mentioned that the physical dimensions computed above could be considered as initial dimensions for the pyramidal horn antenna which will be shown in the following section.

3. SIMULATED DESIGN

3.1 DESIGN I

In this section, the design of a pyramidal horn antenna operating at X- and Ku- band frequencies is presented using the CST microwave studio. The physical dimensions of the antenna computed in section 2.1 is inserted into the CST and utilised to

design the antenna as shown in Fig. 2. The input port is based on the waveguide standard structure WR-90 with dimensions ($a = 22.86 \text{ mm}$, $b = 10.16 \text{ mm}$). The aperture is flared out in both E - and H -planes with dimensions (a_e and a_h). The dimensions values of the aperture are computed using the analysis discussed in Section 2.

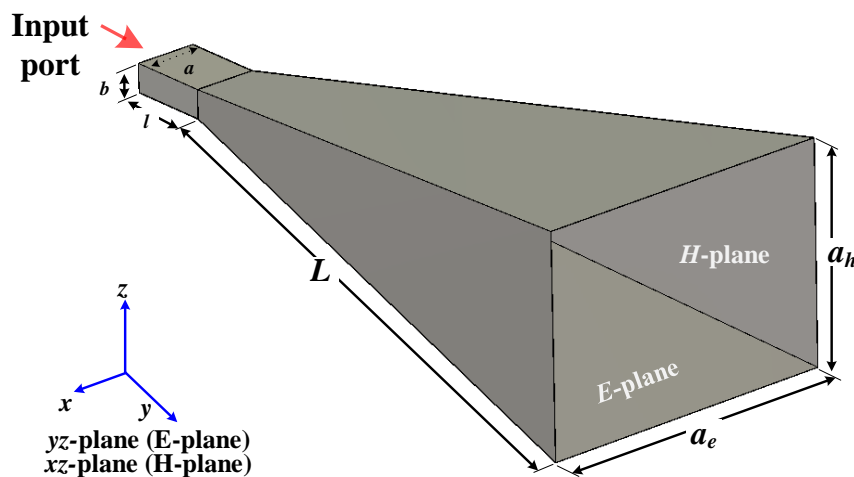


Figure 2: Pyramidal horn antenna (Design I) based on waveguide structure modeled in CST. The dimensions in mm are: $a_e = a_h = 59.12$, $L = 46.14$, $l = 10.16$, $a = 22.86$, $b = 10.16$.

The simulated results of the conventional horn antenna are obtained from the CST simulator. Fig. 3 shows the return loss (S11) variation versus frequencies. It can be seen there is a very good impedance matching (below -10 dB) from 8.3 GHz to 15 GHz. The impedance bandwidth at the centre frequency $f_0 = 13$ GHz is 51.5 %. It is important to mention that the material used in the

antenna design is perfect electrical conductor (PEC). The variation of the realised gain (including the losses due to the mismatch and material) is shown in Fig. 4. The peak gain, which is 13.49 dBi, is depicted at 14.5 GHz. The antenna radiation patterns are shown in Fig. 5. They are relatively directive with very low side lobe levels.

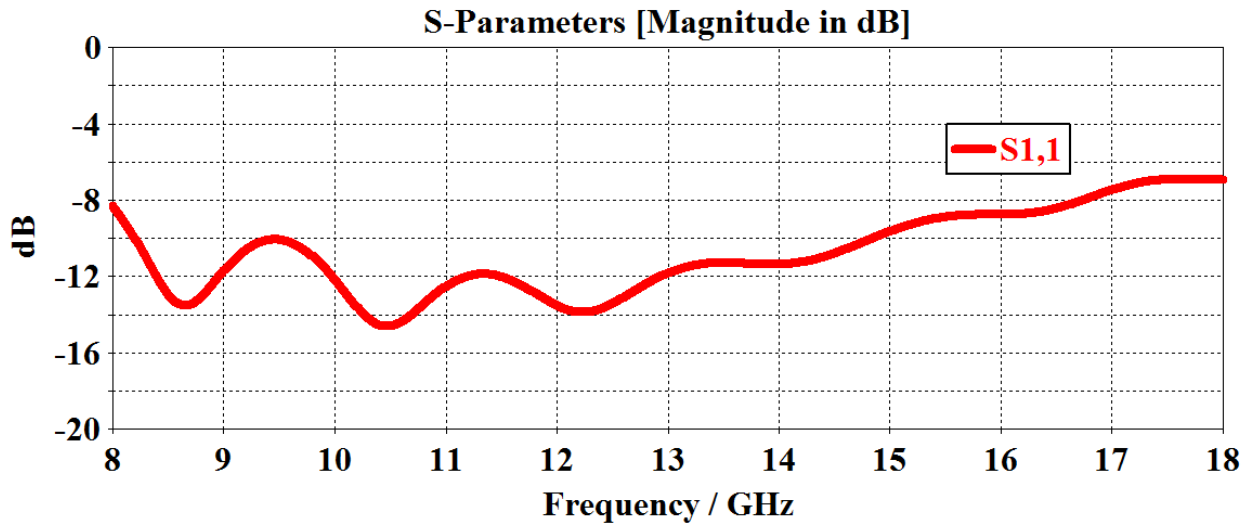


Figure 3: The return loss variation versus operating frequencies band.

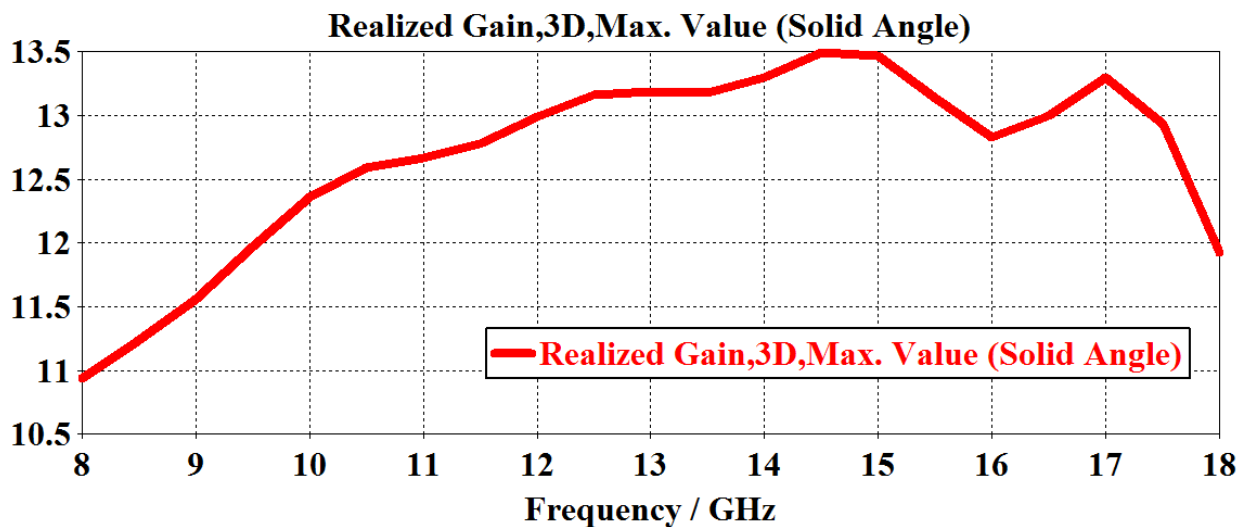
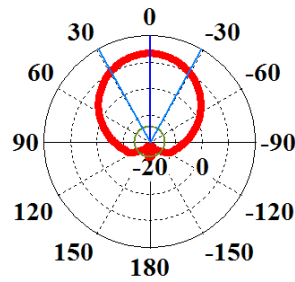


Figure 4: The realised gain variation versus operating frequencies band.

Farfield Realized Gain Abs (Phi=90)



Theta / Degree vs. dBi

Frequency = 13 GHz

Main lobe magnitude = 13.2 dBi

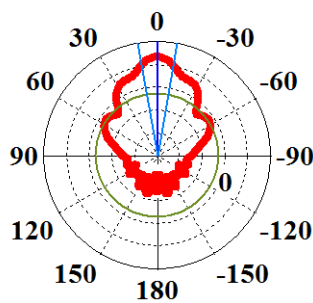
Main lobe direction = 0.0 deg.

Angular width (3 dB) = 58.3 deg.

Side lobe level = -27.2 dB

(a)

Farfield Realized Gain Abs (Phi=0)



Theta / Degree vs. dBi

Frequency = 13 GHz

Main lobe magnitude = 13.2 dBi

Main lobe direction = 0.0 deg.

Angular width (3 dB) = 20.0 deg.

Side lobe level = -15.8 dB

(b)

Figure 5: The radiation patterns in *E*- and *H*- planes at 13 GHz.

3.2 Design II

In this section, the design of a pyramidal horn antenna with a metasurface, which bears a set of identical periodic unit cell, is demonstrated. As shown in Fig. 6 (a), the periodic unit cells are employed on the both sides of the E-plane. The unit cell dimensions are optimised using the Genetic algorithm in the CST in order to enhance the reflection coefficient and bandwidth. The optimisation process begins by defining the dimensions of the unit cell which must be smaller than the operating wavelength (λ). As can be seen in Fig. 6 (b), the top side of the unit cell consists of a microstrip layer with cutting eight patches out of it. The microstrip layer is placed on a substrate

with a relative permittivity of 4.3. After the optimisation process is complete, the horn antenna is simulated including the optimised unit cells. This is to verify the influence of the unit cells on the antenna performance. Fig. 7 shows the S_{11} variation of the horn antenna with metasurface layer versus frequencies. One can notice that the antenna has good impedance matching at the start and stop bands. However, around the centre band, the S_{11} is degraded. It has been found that this is due to the non-resonating structure of the unit cells. Similarly, the antenna realised gain is also degraded around the centre frequency as shown in Figure 8. This is due to the loss occurred as a result of mismatch. However, significant realised gain improvement (~ 10 dBi) can be noticed at the start and stop bands when comparing with the antenna response without the metasurface as presented in Fig. 4.

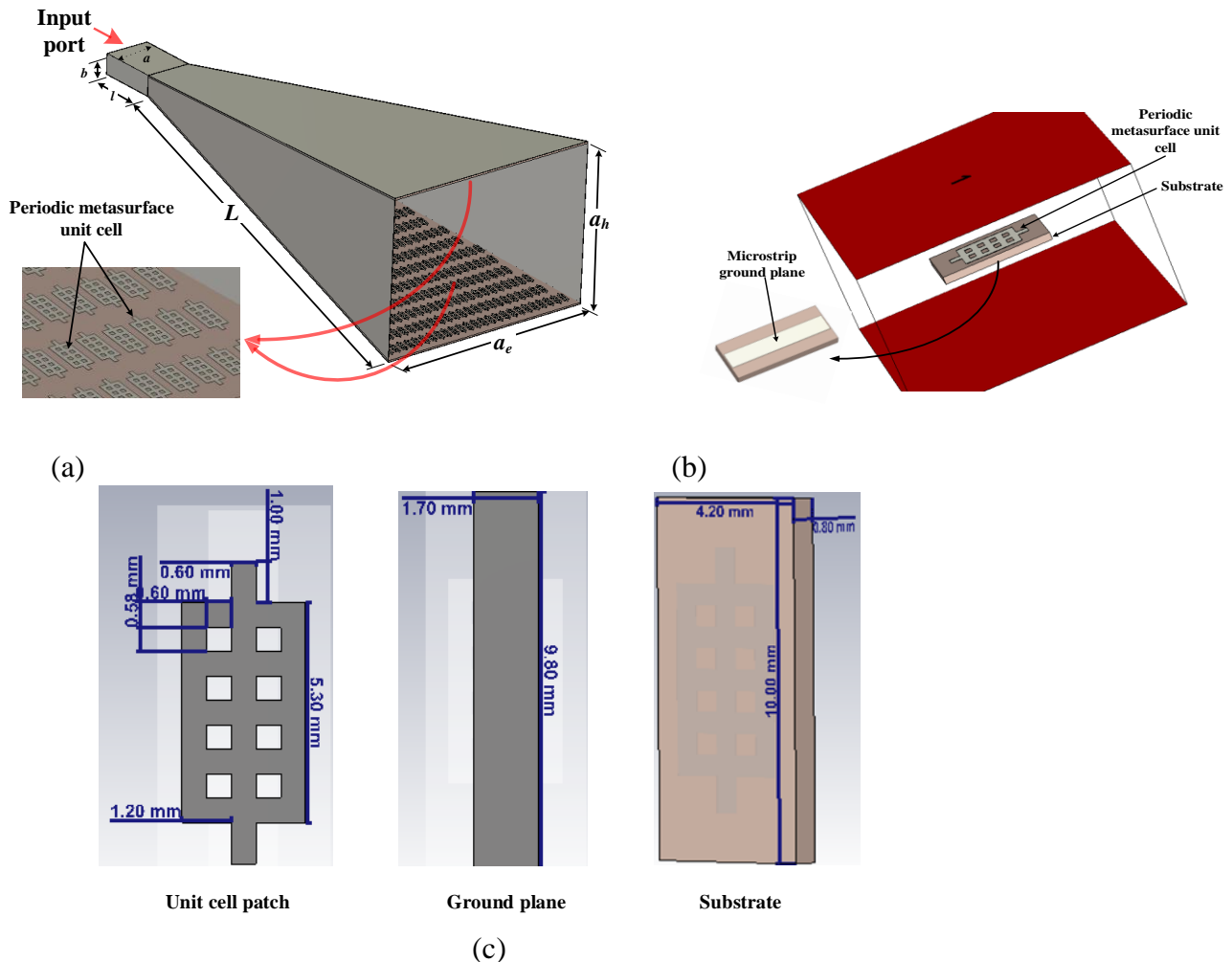


Figure 6: (a) Pyramidal horn with metasurface layers (Design II) placed at both sides of the E -plane. The dimensions in mm are: $a_e = a_h = 59.12$, $L = 46.14$, $l = 10.16$, $a = 22.86$, $b = 10.16$. (b) Layout of a single unit cell. (c) dimensions of the unit cell.

The peak gain is 23.7 dBi at 13 GHz. Although, the side lobe level is relatively increased in the E -plane, significant side lobe level reduction is achieved in the H -plane as can be observed in Fig. 9. For better clarifications, Table 1 compares the fundamental electrical properties of the horn antenna obtained by; 1) calculations, 2) CST simulation without metasurface layer, and 3) CST simulation with metasurface layer. It is concluded from the table that, in terms of gain and radiation patterns, design

2 is preferred over the other designs. It is worth mentioning that design 2 is low profile and such performance could be of interest in some satellite applications.

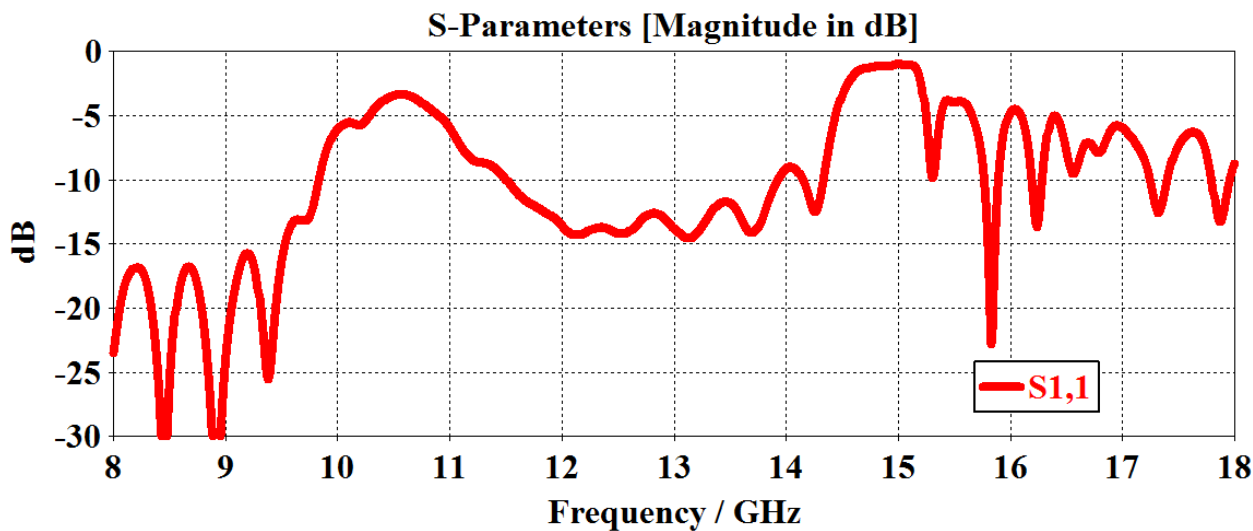


Figure 7: The return loss variation versus operating frequencies band.

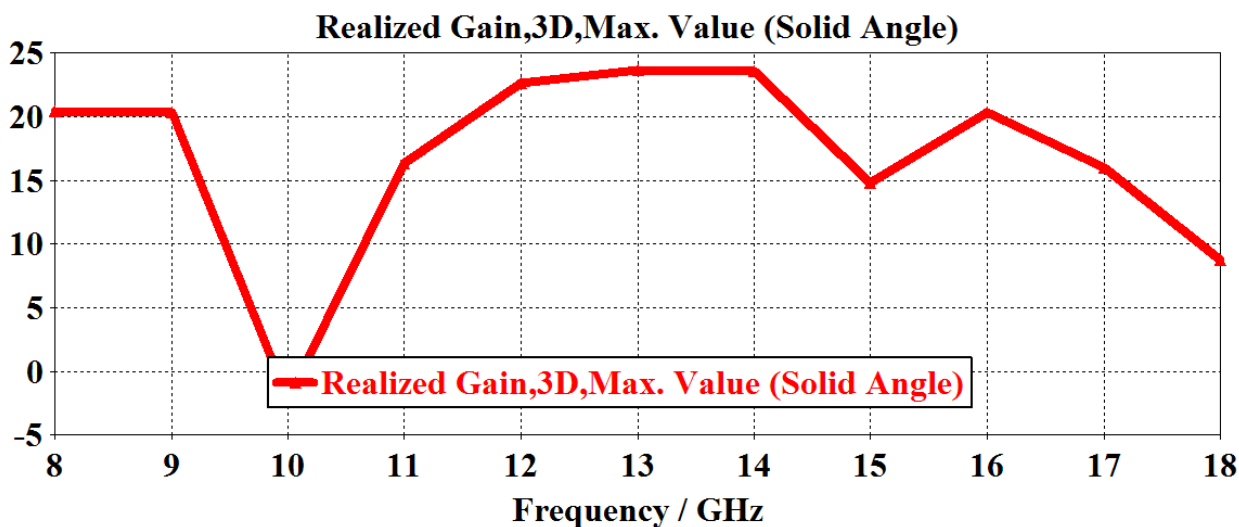
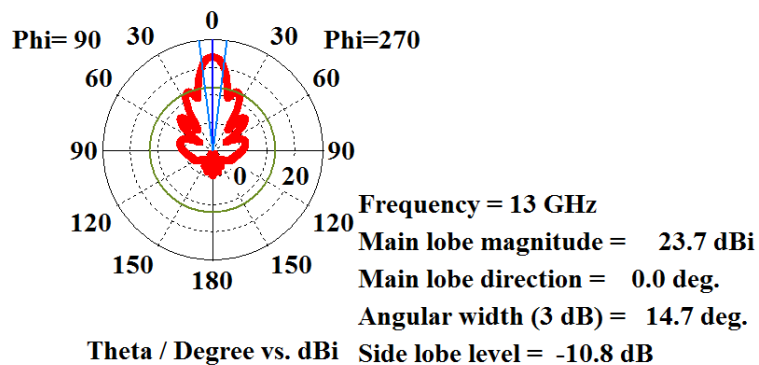


Figure 8: The realised gain variation versus operating frequencies band.

Farfield Realized Gain Abs (Phi=90)



(a)

Farfield Realized Gain Abs (Phi=0)

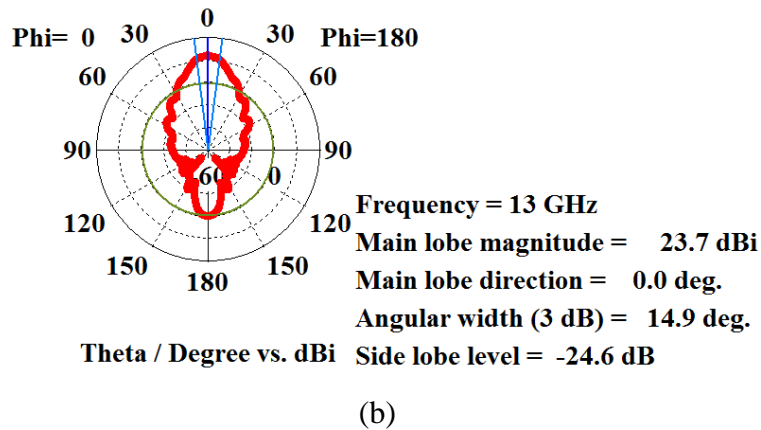
Figure 9: The radiation patterns in E - and H - planes at 13 GHz.

Table 1: Comparison of the electrical properties of the conventional pyramidal horn antenna with the calculations and metasurface based.

Electrical Parameters	Operating frequency	HPBW (Degree)	Directivity (dBi)	Realised gain (dBi)	Bandwidth (%) ($S_{11} = -10$ dB)
Calculations	13 GHz	21.91 ^o	16.92	NA	NA
Design I		E-plane 58.3 ^o H-plane 20.0 ^o	13.25	13.2	51.5
Design II		E-plane 14.7 ^o H-plane 14.9 ^o	23.8	23.7	start band 14.5 stop band 21.3

4.CONCLUSION

A new design of the Pyramidal horn antenna operated in the range frequencies 8-18 GHz was presented in this paper. A metasurface layer which consists of a set of identical periodic unit cells was placed on the both side of the E-plane of the horn. This has improved the gain and bandwidth significantly. With the conventional design analysis presented, the performance of the horn antenna based on the metasurface was improved. The antenna provided wide bandwidth at the start and stop bands. Also, such enhancement was not at the cost of the size. The proposed pyramidal horn antenna is compact which may be of interest in some satellite communication applications.

References

- ABDULKARIM, Y. I., AWL, H. N., MUHAMMADSHARIF, F. F., KARAASLAN, M., MAHMUD, R. H., HASAN, S. O., IŞIK, Ö., LUO, H. & HUANG, S. 2020. A low-profile antenna based on single-layer metasurface for Ku-band applications. *International Journal of Antennas and Propagation*.
- ASL, A. N., YOUSIF, B. & AL-ZALABANI, M. 2020. Design, modeling, and fabrication of a new compact perfect metamaterial X-band absorber. *AIP Advances*, 10, 025328.
- CHEN, H.-T., TAYLOR, A. J. & YU, N. 2016. A review of metasurfaces: physics and applications. *Reports on progress in physics*, 79, 076401.
- CHEN, X. & GE, Y. 2017. Enhancing the radiation performance of a pyramidal horn antenna by

- loading a subwavelength metasurface. *IEEE Access*, 5, 20164-20170.
- CHU, L. & BARROW, W. 1939. Electromagnetic horn design. *Electrical Engineering*, 58, 333-338.
- ESSELLE, K. P. 2007. A low-profile compact microwave antenna with high gain and wide bandwidth. *IEEE transactions on antennas and propagation*, 55, 1880-1883.
- GE, Y., LIN, C. & LIU, K 2018. A Metasurfaced Pyramidal Horn Antenna for Circularly-Polarized Applications. *IEEE Asia-Pacific Conference on Antennas and Propagation (APCAP)*, IEEE, 517-518.
- GE, Y., SUN, Z., CHEN, Z. & CHEN, Y.-Y. 2016. A high-gain wideband low-profile Fabry-Pérot resonator antenna with a conical short horn. *IEEE Antennas and Wireless Propagation Letters*, 15, 1889-1892.
- LI, Y., GE, L., WANG, J., DA, S., CAO, D., WANG, J. & LIU, Y. 2019. 3-D printed high-gain wideband waveguide fed horn antenna arrays for millimeter-wave applications. *IEEE Transactions on Antennas and Propagation*, 67, 2868-2877.
- LIER, E. & SHAW, R. 2008. Design and simulation of metamaterial-based hybrid-mode horn antennas. *Electronics letters*, 44, 1444-1445.
- LIN, C., GE, Y., BIRD, T. S. & LIU, K. 2018. Circularly polarized horns based on standard horns and a metasurface polarizer. *IEEE Antennas and Wireless Propagation Letters*, 17, 480-484.
- MARHEFKA, R. J. & KRAUS, D. 2002. Antennas for all Applications. *Antennas for all applications*.
- MAYBELL, M. J. & SIMON, P. S. 1993. Pyramidal horn gain calculation with improved accuracy. *IEEE transactions on antennas and propagation*, 41, 884-889.
- MORADI, A. & MOHAJERI, F. 2017. Side lobe level reduction and gain enhancement of a pyramidal horn antenna in the presence of metasurfaces. *IET Microwaves, Antennas & Propagation*, 12, 295-301.
- PAN, B., LI, Y., PONCHAK, G. E., PAPAPOLYMEROU, J. & TENTZERIS, M. M. 2009. A 60-GHz CPW-fed high-gain and broadband integrated horn antenna. *IEEE Transactions on Antennas and Propagation*, 57, 1050-1056.
- WANG, P., WU, Q., HE, R.-B. & LUO, W. 2019. Gain and radiation pattern enhancement of the H-plane horn antenna using a tapered dielectric lens. *IEEE Access*, 7, 69101-69107.
- WU, Q., SCARBOROUGH, C. P., GREGORY, M. D., WERNER, D. H., SHAW, R. K. & LIER, E. Broadband metamaterial-enabled hybrid-mode horn antennas. 2010 *IEEE Antennas and Propagation Society International Symposium*. IEEE, 1-4.
- WU, Q., SCARBOROUGH, C. P., WERNER, D. H., LIER, E. & SHAW, R. K. 2013. Inhomogeneous metasurfaces with engineered dispersion for broadband hybrid-mode horn antennas. *IEEE transactions on antennas and propagation*, 61, 4947-4956.
- WU, Q., SCARBOROUGH, C. P., WERNER, D. H., LIER, E. & WANG, X. 2012. Design synthesis of metasurfaces for broadband hybrid-mode horn antennas with enhanced radiation pattern and polarization characteristics. *IEEE transactions on antennas and propagation*, 60, 3594-3604.